JOURNAL SYNTAX IDEA
p–ISSN: 2723-4339 e-ISSN: 2548-1398
Vol. 8, No. 8, August 2026

Comparative Study of Structural, Thermal, and Tensile Characterization of Material-Extrusion-Printed Recycled PLA and Recycled HDPE

Muhammad Satya Putra Gantada[1]*, Haruhi Mochizuki[2], Julia Ananda Puteri[3], Kim SooBong[4]
Korea Advanced Institute of Science and Technology, Korea[1]
Universitas Sriwijaya, Indonesia[2]
Gakushuin University, Tokyo[3]
Seoul National University, Korea[4]
Email: gantasatya51@gmail.com[1]*

Keywords:
recycled PLA; recycled HDPE; material extrusion; thermal stability; crystallinity; tensile properties.

Abstract

The increasing use of recycled polymers in additive manufacturing requires a clear understanding of how molecular structure and thermal behavior influence mechanical performance. This study comparatively evaluated material-extrusion-printed recycled polylactic acid (rPLA) and recycled high-density polyethylene (rHDPE) using Fourier-transform infrared spectroscopy (FTIR), X-ray diffraction (XRD), thermogravimetric analysis (TGA), derivative thermogravimetry (DTG), differential scanning calorimetry (DSC), and tensile testing. FTIR analysis confirmed that both materials retained their primary polymer structures after processing, although weak oxygen-containing bands in rHDPE suggested limited thermo-oxidative modification. XRD analysis revealed that rPLA exhibited a predominantly amorphous structure with a broad diffraction halo at 16.17°, whereas rHDPE maintained distinct orthorhombic crystalline reflections at 21.58° and 23.96°. Thermal analysis demonstrated that rHDPE had substantially higher thermal degradation resistance, with the maximum degradation rate occurring at approximately 470–480 °C compared with 350–360 °C for rPLA. DSC analysis further identified cold crystallization and melting transitions in rPLA, while rHDPE exhibited a pronounced melting transition consistent with its semicrystalline structure. Mechanically, rPLA demonstrated higher tensile strength and Young's modulus, reaching 55.528 MPa and 3.176 GPa, respectively, whereas rHDPE exhibited substantially higher elongation at break (72.667%). All measured differences were statistically significant ($p < 0.0001$). These findings demonstrate that rPLA is more suitable for rigid, load-bearing printed components, whereas rHDPE is more appropriate for applications requiring flexibility and extensive plastic deformation. The results support application-specific material selection rather than direct substitution between recycled polymers in circular material-extrusion-based manufacturing.

INTRODUCTION

Material-extrusion additive manufacturing has expanded rapidly because it enables the production of complex components with relatively low material waste, accessible

equipment, and flexible design modification. However, the increasing consumption of thermoplastic filaments also generates rejected prints, support structures, and end-of-life components that may reduce the environmental benefits of additive manufacturing when these materials are not recovered (Bergaliyeva et al., 2023). Mechanical recycling provides a practical pathway for converting polymer waste into reusable feedstock; however, repeated heating, extrusion, and solidification processes can alter molecular organization, thermal stability, crystallization behavior, and mechanical performance (Agbakoba et al., 2024). Therefore, the suitability of recycled polymers for 3D printing cannot be evaluated solely based on their ability to pass through the printer nozzle; their chemical, structural, thermal, and mechanical characteristics must also be comprehensively assessed. Recent studies have emphasized the recovery and reuse of polymer waste as an important strategy for developing more circular additive manufacturing systems (Agbakoba et al., 2024; Hasan et al., 2024).

Recycled polylactic acid (rPLA) is particularly attractive because PLA is widely used in material extrusion processes and is derived from renewable feedstocks. Nevertheless, its ester-containing polymer backbone is susceptible to thermal and hydrolytic degradation during reprocessing, which may reduce molecular weight and alter melt behavior (Bergaliyeva et al., 2023). The rapid cooling associated with layer-by-layer deposition can also limit chain rearrangement, often resulting in a predominantly amorphous or weakly ordered structure in printed PLA. This thermal history influences subsequent cold crystallization, melting behavior, stiffness, and failure strain (Hasan et al., 2024). Although recycled PLA can maintain sufficient mechanical strength for printed components, its final performance remains dependent on the number of processing cycles, filament production conditions, and printing parameters (Lendvai et al., 2025).

Recycled high-density polyethylene (rHDPE) represents a contrasting polymer system. Its nonpolar methylene backbone and regular chain structure promote the formation of an orthorhombic semicrystalline phase, resulting in thermal and mechanical characteristics that differ substantially from those of PLA. Previous studies have demonstrated the feasibility of recovering HDPE waste for additive manufacturing while showing that recycled HDPE retains significant crystalline ordering and high tensile deformability (Daniele et al., 2023). Its higher degradation temperature provides a wider processing window between melting and thermal decomposition; however, its rapid crystallization and high chain mobility can influence shrinkage and dimensional stability during cooling. From a mechanical perspective, polyethylene crystallites function as physical crosslinks, while flexible amorphous chains enable yielding, chain sliding, and extensive plastic deformation under tensile loading (Yong Quek et al., 2025).

Although rPLA and rHDPE have each been investigated as recycled feedstocks for material extrusion, direct comparisons between these materials have often been limited to printability assessments or individual mechanical properties. A comprehensive evaluation of their chemical structures, crystalline organization, degradation behavior, thermal transitions, and tensile responses is required to clarify why these polymers exhibit different performances after printing (Abinda & Gantada, 2025). Such comparisons are

particularly important because higher crystallinity does not necessarily result in greater stiffness or strength when polymers possess fundamentally different backbone structures and molecular mobility. Establishing structure–thermal–property relationships can therefore provide a more reliable basis for selecting recycled materials according to specific functional requirements rather than treating them as interchangeable alternatives.

The urgency of this research is driven by the increasing volume of polymer waste generated from additive manufacturing and the growing demand for sustainable feedstock alternatives. As the 3D printing industry continues to expand, the accumulation of rejected prints and end-of-life components presents an environmental challenge that mechanical recycling can help mitigate. However, without a comprehensive understanding of how recycling and printing processes affect material properties, the adoption of recycled polymers for functional applications remains limited. This study contributes to addressing this knowledge gap by providing empirical evidence that supports material selection in circular manufacturing systems.

Accordingly, this study comparatively investigated material-extrusion-printed rPLA and rHDPE using Fourier-transform infrared spectroscopy (FTIR), X-ray diffraction (XRD), thermogravimetric analysis (TGA), derivative thermogravimetry (DTG), differential scanning calorimetry (DSC), and tensile testing. The analysis focused on identifying characteristic functional groups, molecular ordering, thermal degradation behavior, phase transitions, and deformation characteristics. By integrating these results, the study aimed to determine how the glassy, predominantly amorphous structure of rPLA and the flexible semicrystalline structure of rHDPE governed their respective balance among strength, stiffness, thermal resistance, and ductility. The findings are expected to support application-specific material selection and contribute to the development of circular material-extrusion manufacturing using recycled thermoplastics.

METHOD

Recycled polylactic acid (rPLA) and recycled high-density polyethylene (rHDPE) specimens produced through material-extrusion 3D printing were comparatively evaluated to determine their chemical, structural, thermal, and mechanical characteristics. Fourier-transform infrared spectroscopy (FTIR) was used to identify characteristic functional groups and potential chemical modifications associated with recycling and thermal processing, while X-ray diffraction (XRD) was employed to analyze molecular ordering and crystalline structures. Thermal stability and decomposition behavior were evaluated using thermogravimetric analysis (TGA) and derivative thermogravimetry (DTG), whereas differential scanning calorimetry (DSC) was performed to assess glass transition, cold crystallization, melting behavior, and crystallinity differences. Tensile testing was subsequently conducted to obtain stress–strain curves, tensile strength, elongation at break, and Young's modulus. The results from these characterization techniques were integrated to establish relationships among polymer structure, thermal response, and tensile performance of the material-extrusion-printed recycled polymers.

RESULTS AND DISCUSSION

Chemical and Structural Characteristics Analysis

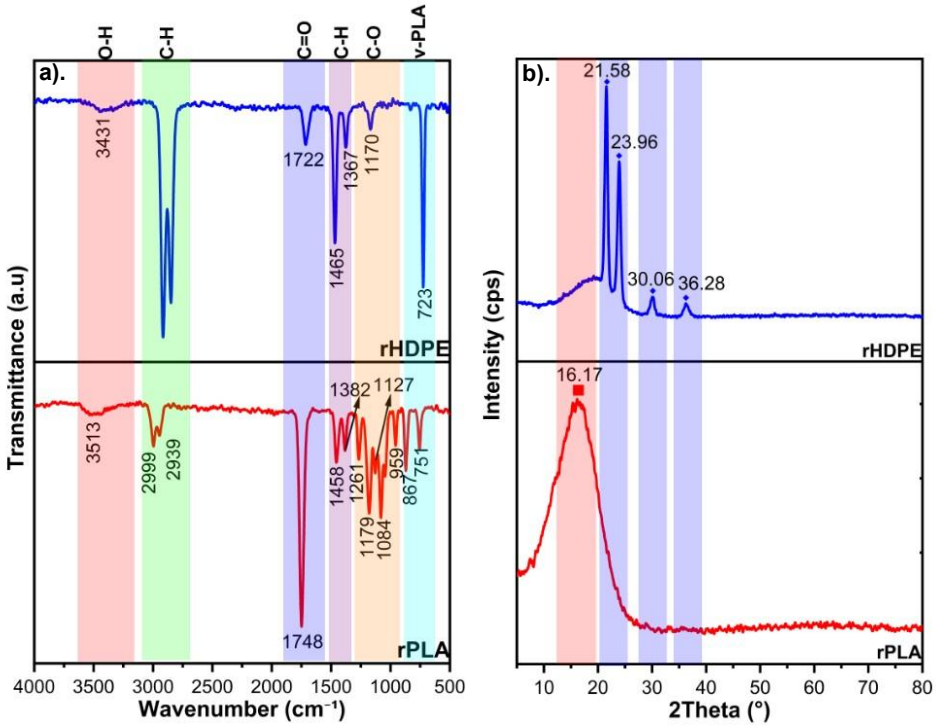

Figure 1. FTIR spectra and XRD patterns of material-extrusion-printed rPLA and rHDPE

Figure 1a compares the FTIR spectra of material-extrusion-printed recycled PLA (rPLA) and recycled HDPE (rHDPE). The rPLA spectrum retains the characteristic chemical signature of an aliphatic polyester. The weak band at 3513 cm^{-1} can be associated with terminal hydroxyl groups and/or adsorbed moisture, whereas the bands at 2999 and 2939 cm^{-1} correspond to asymmetric and symmetric C–H stretching vibrations, respectively (Chopra et al., 2023). The intense absorption at 1748 cm^{-1} is assigned to the stretching vibration of the ester carbonyl group, representing the principal spectroscopic feature of PLA. The bands at 1458 and 1382 cm^{-1} originate predominantly from CH_3 bending and deformation, while the group of bands at 1261, 1179, 1127, 1084, and 1045 cm^{-1} is associated with C–O–C and C–O stretching within the ester backbone (Erdem et al., 2025). The lower-wavenumber bands at 867 and 751 cm^{-1} are related to PLA skeletal vibrations, C–C backbone stretching, and C–H rocking modes that are sensitive to chain conformation and structural ordering (Yan et al., 2023).

In contrast, the rHDPE spectrum is dominated by the vibrations of its methylene-rich hydrocarbon backbone. The strong absorption doublet in the 3000–2800 cm^{-1} region is attributed to asymmetric and symmetric CH_2 stretching, while the bands at 1465 and 1367 cm^{-1} correspond to CH_2 scissoring and C–H deformation modes. The intense band at 723 cm^{-1} is assigned to the rocking vibration of consecutive methylene units and is characteristic of ordered polyethylene chains (Khozemy et al., 2023). The preservation of

these dominant bands confirms that the polyethylene backbone remains the principal chemical structure of the recycled material. The comparatively weak absorptions at 3431, 1722, and 1170 cm^{-1} are not intrinsic dominant bands of pristine HDPE. The 1722 cm^{-1} band is consistent with carbonyl-containing species generated by limited thermo-oxidative degradation, while the broad 3431 cm^{-1} contribution may originate from adsorbed moisture or hydroxyl-containing oxidation products (Aravind et al., 2021). The 1170 cm^{-1} band may similarly reflect C–O-containing oxidation products or residual additives from the original HDPE waste stream. Nevertheless, their low intensities relative to the CH_2 bands suggest that oxidation was limited rather than sufficiently severe to obscure the original polyethylene structure (Chrysafi et al., 2022).

The XRD patterns in Figure 1b reveal a pronounced difference in molecular ordering between the two recycled polymers. The rPLA sample exhibits a broad diffraction halo centered at $2\theta = 16.17°$, without clearly resolved sharp reflections. This profile indicates a predominantly amorphous or weakly ordered structure, which is commonly observed when PLA undergoes rapid cooling during material extrusion and insufficient time is available for extensive chain rearrangement and crystal growth (Nejatpour et al., 2025). Therefore, the feature at 16.17° should be interpreted primarily as an amorphous halo rather than as evidence of a highly developed PLA crystalline phase (Tănase et al., 2024).

Conversely, rHDPE presents sharp and intense diffraction peaks at $2\theta = 21.58°$ and 23.96°, corresponding to the (110) and (200) planes of the orthorhombic polyethylene crystal structure. The weaker reflections at 30.06° and 36.28° are consistent with higher-order reflections of ordered polyethylene, with the latter commonly indexed to the (020) plane (Tarani et al., 2023). The narrow and well-defined peaks confirm that rHDPE retains substantial semicrystalline ordering despite its previous service life, recycling history, filament extrusion, and subsequent 3D printing. Recent investigations similarly report the principal orthorhombic HDPE reflections at approximately 21.5°, 23.9°, and 36.2° (Farashiani et al., 2024; Ullah & Ali, 2025).

Taken together, FTIR and XRD demonstrate that the two materials preserve their expected polymer-specific structures after material extrusion while exhibiting fundamentally different levels of molecular organization. The ester-rich rPLA structure is associated with a broad, predominantly amorphous diffraction profile, whereas the regular methylene sequence of rHDPE facilitates efficient chain packing and produces pronounced orthorhombic crystalline reflections. The weak oxygen-containing FTIR bands in rHDPE indicate limited oxidation associated with recycling or thermal processing, but the persistence of its characteristic XRD pattern shows that this chemical modification did not eliminate the principal crystalline organization. These structural differences provide an essential basis for interpreting the subsequent DSC crystallization behavior, thermal degradation profiles, and tensile response of the printed polymers.

Thermal Behavior and Stability Analysis

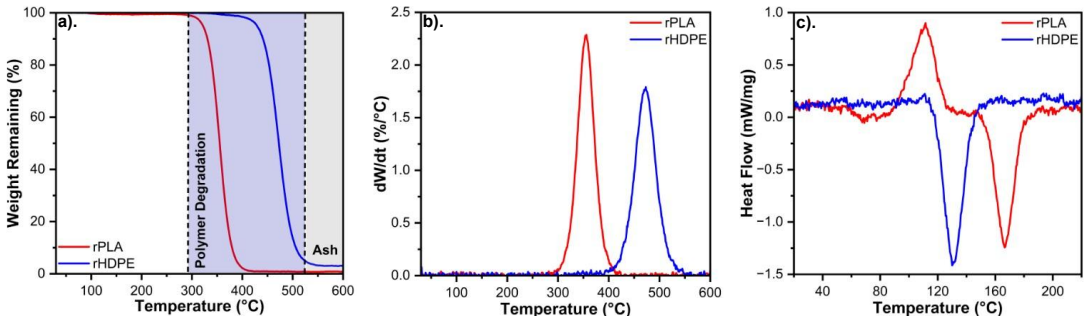

Figure 2. Thermal characteristics of rPLA and rHDPE: (a) TGA, (b) DTG, and (c) DSC curves

The thermal behavior of material-extrusion-printed rPLA and rHDPE was evaluated using TGA, DTG, and DSC, as presented in Figure 2. Both polymers exhibit relatively stable mass profiles at low and intermediate temperatures, followed by a dominant single-step degradation process. However, their decomposition intervals differ substantially. The rPLA curve begins to decrease at approximately 300 °C and undergoes rapid mass loss between approximately 320 and 390 °C. In comparison, rHDPE maintains its initial mass to a markedly higher temperature, with its principal degradation occurring at approximately 410–510 °C. This displacement toward higher temperatures demonstrates that rHDPE possesses greater thermal stability than rPLA under the applied testing conditions (Bergaliyeva et al., 2023). The lower decomposition temperature of rPLA is associated with the comparatively thermally sensitive ester-containing backbone, whereas the hydrocarbon structure of rHDPE requires higher thermal energy for extensive chain scission and volatilization. Similar differences between thermally processed PLA and recycled HDPE have been reported in recent investigations of recycled polymers for extrusion-based manufacturing (Agbakoba et al., 2024; Martínez et al., 2024).

The DTG curves in Figure 2b further confirm the predominantly single-stage degradation of both materials. The maximum degradation-rate temperature, Tmax, is located at approximately 350–360 °C for rPLA and 470–480 °C for rHDPE, consistent with the inflection regions of the corresponding TGA curves. The narrow rPLA peak indicates rapid decomposition over a relatively limited temperature interval, which is characteristic of extensive chain cleavage and depolymerization after thermal degradation begins. By contrast, the rHDPE peak occurs at a considerably higher temperature and is slightly broader, indicating that the principal fragmentation and volatilization of the polyethylene backbone require greater thermal input (Martínez et al., 2024). Recycled HDPE processed through extrusion has similarly been reported to exhibit a principal DTG maximum near 485 °C and almost complete conversion into volatile degradation products.

Both samples leave only negligible residual mass near 600 °C. This suggests that the materials contain a low proportion of nonvolatile inorganic constituents under the test atmosphere (Daniele et al., 2023). Nevertheless, the small residual fraction should not be

used alone to conclude that the recycled polymers are completely free from additives or contamination, because organic additives may also volatilize during thermal decomposition (Martínez et al., 2024). The near-complete degradation of rHDPE is consistent with recent thermal analyses of mechanically recycled HDPE, whereas recycled PLA formulations may also present low final residue when they do not contain substantial mineral reinforcement (Bergaliyeva et al., 2023).

The DSC thermograms in Figure 2c reveal distinct thermal-transition and crystallization behaviors. The rPLA curve exhibits a weak baseline change in the approximate glass-transition region of 50–70 °C, followed by a pronounced exothermic peak near 110 °C and an endothermic melting peak at approximately 165–170 °C. The exothermic event is attributed to cold crystallization, indicating that a considerable fraction of the rPLA chains remained in a kinetically constrained amorphous state after material extrusion and subsequently reorganized into more ordered domains during DSC heating (Portoacă et al., 2024). The melting endotherm then represents the disruption of the crystalline structures present before heating and those formed during cold crystallization. This behavior is consistent with recycled and material-extruded PLA, for which rapid cooling during printing can restrict crystallization and produce a pronounced cold-crystallization response during subsequent heating (Agbakoba et al., 2024; Bergaliyeva et al., 2023).

In contrast, rHDPE displays a dominant endothermic melting peak at approximately 125–135 °C without a pronounced cold-crystallization event. This response reflects the ability of the relatively regular polyethylene chains to crystallize readily during cooling after extrusion. The sharp melting endotherm agrees with the semicrystalline structure identified by the strong orthorhombic XRD reflections at 21.58° and 23.96°. Recent characterization of processed recycled HDPE has similarly reported a melting temperature around 130–137 °C, depending on the source, thermal history, and degree of contamination of the recycled feedstock (Daniele et al., 2023; Martínez et al., 2024).

The combined XRD and DSC results therefore establish a consistent structural interpretation. The broad rPLA XRD halo and its pronounced DSC cold-crystallization peak indicate a predominantly amorphous as-printed state with latent crystallization capability. Conversely, the sharp rHDPE diffraction peaks and single well-defined melting endotherm demonstrate substantial semicrystalline organization developed during cooling (Shanmugam et al., 2024). Moreover, the decomposition temperatures of both materials remain substantially above their melting transitions, indicating a usable thermal interval between melting and bulk degradation during material extrusion. This interval is wider for rHDPE, although its practical processing behavior may still be constrained by melt viscosity, shrinkage, and rapid crystallization rather than thermal decomposition alone (Hasan et al., 2024b).

Quantitative crystallinity should only be calculated when the integrated melting and cold-crystallization enthalpies are available. For rPLA, the cold-crystallization enthalpy must be subtracted from the melting enthalpy, whereas the rHDPE crystallinity can be estimated from its melting enthalpy using an appropriate value for fully crystalline HDPE.

Mechanical Properties Analysis

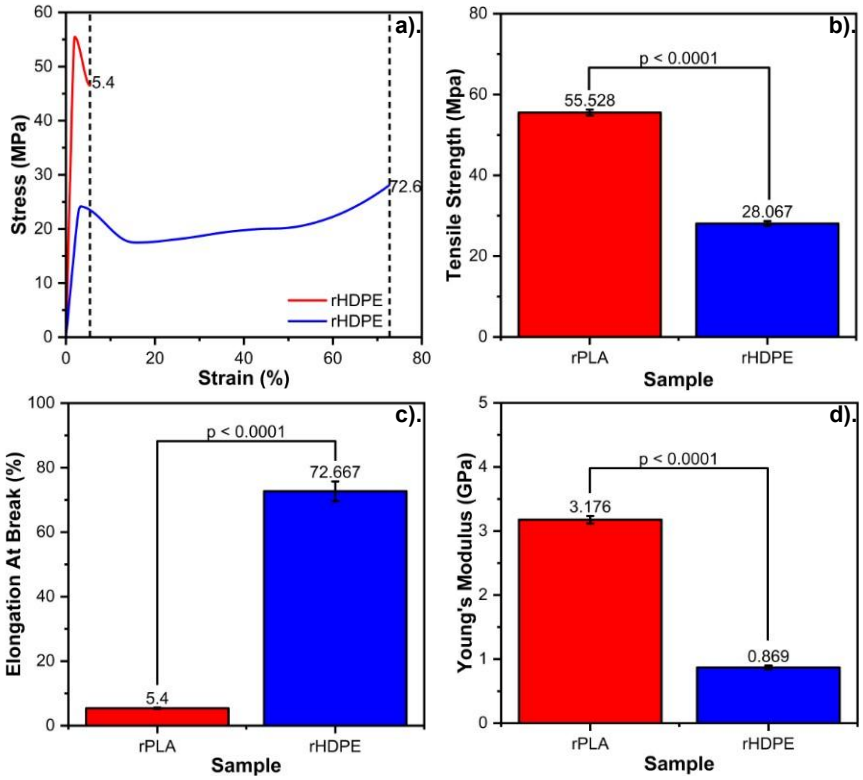

Figure 3. Tensile properties of rPLA and rHDPE: (a) stress–strain curves, (b) tensile strength, (c) elongation at break, and (d) Young's modulus

Figure 3 compares the tensile behavior of material-extrusion-printed rPLA and rHDPE. The stress–strain curves reveal two distinctly different deformation responses. The rPLA specimen exhibits a steep, nearly linear increase in stress followed by abrupt failure at approximately 5.4% strain, indicating a stiff but relatively brittle response with limited plastic deformation. In contrast, rHDPE initially reaches a yield stress of approximately 24 MPa, followed by a reduction toward a stable plastic-flow region (Bartczak & Vozniak, 2024). The stress subsequently increases again at large deformation before failure at approximately 72.6% strain. This sequence is characteristic of yielding, localized necking or cold drawing, and strain hardening in semicrystalline polyethylene. Similar deformation stages have been associated with lamellar slip, fragmentation, and progressive molecular-chain orientation during tensile loading of HDPE (Kida et al., 2022).

Quantitatively, rPLA achieved a tensile strength of 55.528 MPa, almost twice that of rHDPE at 28.067 MPa. The Young's modulus of rPLA was also substantially higher, reaching 3.176 GPa compared with 0.869 GPa for rHDPE. Thus, rPLA was approximately 3.65 times stiffer than rHDPE. Conversely, rHDPE exhibited an elongation at break of 72.667%, approximately 13.5 times the 5.4% recorded for rPLA. All three parameters differed significantly between the materials at $p<0.0001$. The tensile strength and modulus obtained for rPLA are within the range recently reported for

material-extrusion-printed PLA, for which tensile strengths of approximately 50–60 MPa and moduli near 3 GPa have been observed depending on feed rate, layer geometry, and thermal history (Lendvai et al., 2025).

The superior strength and stiffness of rPLA are consistent with its molecular and thermal characteristics. FTIR confirmed the presence of polar ester and carbonyl groups, while DSC showed that the material remained below its glass-transition region under ambient tensile-testing conditions. Consequently, segmental chain mobility was restricted, producing a high elastic modulus and rapid stress accumulation but limiting deformation before failure. The broad XRD halo of rPLA therefore should not be interpreted as evidence of mechanically soft behavior: although the printed material was predominantly amorphous, its glassy state and comparatively strong intermolecular interactions generated a rigid tensile response. Recent studies of recycled PLA printed by material extrusion similarly report tensile strengths strongly dependent on processing history, with the material generally retaining a comparatively high stiffness despite variations caused by recycling and printing conditions (Hasan et al., 2024).

Although rHDPE displayed stronger crystalline reflections than rPLA, its modulus and tensile strength were lower. This result demonstrates that a higher degree of crystalline ordering does not necessarily produce greater bulk stiffness when polymers with fundamentally different chain structures are compared. The nonpolar and flexible methylene backbone of rHDPE permits extensive chain rotation and sliding within its amorphous regions. Meanwhile, its polyethylene crystallites function as physical junctions that initially resist deformation but can progressively rotate, slip, and reorganize after yielding. These mechanisms explain the long plastic-flow region and the subsequent increase in stress at high strain. Recent work on fused-filament-fabricated rHDPE likewise confirms that recycled polyethylene can retain substantial tensile deformability, although its strength and modulus depend on the recycling history, filament geometry, and printing conditions (Yong Quek et al., 2025).

Taken together, the tensile results establish a clear trade-off between rigidity and deformability. rPLA provides substantially greater strength and stiffness but fails after relatively limited extension, whereas rHDPE accommodates extensive plastic deformation at a lower stress level. These differences are consistent with the preceding FTIR, XRD, and DSC findings: the glassy ester-based structure of rPLA favors load resistance, while the flexible semicrystalline polyethylene structure of rHDPE facilitates yielding and molecular reorientation. Because no fracture-surface or internal-morphology data were collected, the observed differences should primarily be attributed to polymer structure and thermal state rather than to unverified variations in void content or interlayer adhesion.

CONCLUSION

This study demonstrates that recycled PLA (rPLA) and recycled HDPE (rHDPE) retain distinct and application-relevant characteristics after material-extrusion 3D printing. The FTIR and XRD results confirmed that both polymers preserved their

primary chemical structures, although rHDPE exhibited weak oxygen-containing bands associated with limited oxidation while maintaining its orthorhombic semicrystalline structure. In contrast, rPLA remained predominantly amorphous in the printed state, with the potential to undergo crystallization during subsequent heating. Thermal analysis further showed that rHDPE exhibited a broader thermal stability range and higher degradation temperature, whereas rPLA underwent cold crystallization followed by melting, reflecting the strong influence of processing history on polymer chain organization.

More importantly, the mechanical results demonstrated that the two recycled polymers should not be considered direct substitutes but rather materials suited to different functional requirements. rPLA exhibited substantially higher tensile strength and stiffness, making it more suitable for rigid components requiring dimensional stability and load-bearing capability. Conversely, rHDPE demonstrated significantly higher elongation at break and greater capacity for plastic deformation, making it more appropriate for flexible, impact-resistant, or energy-absorbing applications. Therefore, the practical value of recycled polymers in additive manufacturing depends not on identifying a universally superior material but on matching their molecular structure, thermal behavior, and deformation characteristics with specific service requirements. Overall, both rPLA and rHDPE demonstrate strong potential for circular material-extrusion manufacturing, provided that material selection is guided by the required balance among rigidity, thermal resistance, and ductility.

REFERENCES

Abinda, A. E., & Gantada, M. S. P. (2025). Utilization Of Used Pet, Hdpe, And Pp Plastics As Raw Materials For 3d Printing Filaments: A Comparative Study Of Mechanical Properties And Storage Resistance At Room Temperature. Journal of Comprehensive Science, 4(11), 2996–3014. https://doi.org/10.59188/jcs.v4i11.3714

Agbakoba, V. C., Webb, N., Jegede, E., Phillips, R., Hlangothi, S. P., & John, M. J. (2024). Mechanical Recycling of Waste PLA Generated From 3D Printing Activities: Filament Production and Thermomechanical Analysis. Macromolecular Materials and Engineering, 309(8). https://doi.org/10.1002/mame.202300276

Aravind, R., Sahu, A. K., Brahma, G. S., & Swain, T. (2021). Investigation on the Thermo-Oxidative Degradation of Polyethylene, Poly(vinyl chloride), and Polystyrene Using NiPIm1.5 and NiPIm2 Nanocomposites. ACS Omega, 6(44), 29869–29881. https://doi.org/10.1021/acsomega.1c04358

Bartczak, Z., & Vozniak, A. (2024). Deformation Instabilities and Cavitation in Plastic Deformation of Semicrystalline Polyethylene. Macromolecules, 57(14), 6474–6491. https://doi.org/10.1021/acs.macromol.4c00642

Bergaliyeva, S., Sales, D. L., Delgado, F. J., Bolegenova, S., & Molina, S. I. (2023). Manufacture and Characterization of Polylactic Acid Filaments Recycled from Real Waste for 3D Printing. Polymers, 15(9), 2165. https://doi.org/10.3390/polym15092165

Chopra, S., Pande, K., Puranam, P., Deshmukh, A. D., Bhone, A., Kale, R., Galande, A., Mehtre, B., Tagad, J., & Tidake, S. (2023). Explication of mechanism governing atmospheric degradation of 3D-printed poly(lactic acid) (PLA) with different in-fill pattern and varying in-fill density. RSC Advances, 13(11), 7135–7152. https://doi.org/10.1039/D2RA07061H

Chrysafi, I., Asimakidou, T., Michailidou, G., Xanthopoulou, E., Tziamtzi, C. K., Zamboulis, A., & Bikiaris, D. N. (2022). Characterization of the Thermal, Structural, and Mechanical Properties of Recycled HDPE. Macromolecular Symposia, 405(1). https://doi.org/10.1002/masy.202100224

Daniele, R., Armoni, D., Dul, S., & Alessandro, P. (2023). From Nautical Waste to Additive Manufacturing: Sustainable Recycling of High-Density Polyethylene for 3D Printing Applications. Journal of Composites Science, 7(8), 320. https://doi.org/10.3390/jcs7080320

Erdem, F., Kandemir, H., & Alp, F. B. (2025). Effect of Polycaprolactone, Zinc Oxide, and Poly(ethylene glycol) on the Properties of Polylactic Acid Composite Fibers Obtained by Melt Electrospinning. ACS Omega, 10(1), 1457–1469. https://doi.org/10.1021/acsomega.4c09181

Farashiani, M., Shidpour, R., & Rajabi, M. (2024). Influence of exfoliation method of graphene on physical properties of graphene/High Density Polyethylene nanocomposites: Semiconductor-like electrical conductivity, glass transition, and melting temperature. Polymer Engineering & Science, 64(12), 6171–6191. https://doi.org/10.1002/pen.26979

Hasan, M. R., Davies, I. J., Pramanik, A., John, M., & Biswas, W. K. (2024a). Impact of process parameters on improving the performance of 3D printed recycled polylactic acid (rPLA) components. The International Journal of Advanced Manufacturing Technology, 131(7–8), 3751–3779. https://doi.org/10.1007/s00170-024-13140-7

Hasan, M. R., Davies, I. J., Pramanik, A., John, M., & Biswas, W. K. (2024b). Potential of recycled PLA in 3D printing: A review. Sustainable Manufacturing and Service Economics, 3, 100020. https://doi.org/10.1016/j.smse.2024.100020

Khozemy, E. E., Radi, H., & Mazied, N. A. (2023). Upcycling of waste polyethylene and cement kiln dust to produce polymeric composite sheets using gamma irradiation. Polymer Bulletin, 80(5), 5183–5201. https://doi.org/10.1007/s00289-022-04310-2

Kida, T., Hiejima, Y., Nitta, K., & Yamaguchi, M. (2022). Evaluation of microscopic structural changes during strain hardening of polyethylene solids using In situ Raman, SAXS, and WAXD measurements under step-cycle test. Polymer, 250, 124869. https://doi.org/10.1016/j.polymer.2022.124869

Lendvai, L., Fekete, I., Rigotti, D., & Pegoretti, A. (2025). Experimental study on the effect of filament-extrusion rate on the structural, mechanical and thermal properties of material extrusion 3D-printed polylactic acid (PLA) products. Progress in Additive Manufacturing, 10(1), 619–629. https://doi.org/10.1007/s40964-024-00646-5

Martínez, J. L., Rodríguez Rego, J. M., Cerezo, L. M., Madrigal, M. D. S., & Macías-García, A. (2024). Odour characterisation of recycled HDPE in different washing and processing processes. Environmental Science and Pollution Research, 31(47), 58136–58151. https://doi.org/10.1007/s11356-024-34976-2

Nejatpour, M., Fallah, A., & Koc, B. (2025). Shape Memory PLA/TPU Blend Using High-Speed Thermo-Kinetic Mixing. ACS Omega, 10(1), 193–206. https://doi.org/10.1021/acsomega.4c04338

Portoacă, A.-I., Diniță, A., Tănase, M., Săvulescu, A., Sirbu, E.-E., Călin, C., & Brănoiu, G. (2024). Analyzing Sustainable 3D Printing Processes: Mechanical, Thermal, and Crystallographic Insights. Polymers, 16(10), 1364. https://doi.org/10.3390/polym16101364

Shanmugam, V., Babu, K., Kannan, G., Mensah, R. A., Samantaray, S. K., & Das, O. (2024). The thermal properties of FDM printed polymeric materials: A review. Polymer Degradation and Stability, 228, 110902. https://doi.org/10.1016/j.polymdegradstab.2024.110902

Tănase, M., Portoacă, A. I., Diniță, A., Brănoiu, G., Zamfir, F., Sirbu, E.-E., & Călin, C. (2024). Optimizing Mechanical Properties of Recycled 3D-Printed PLA Parts for Sustainable Packaging Solutions Using Experimental Analysis and Machine Learning. Polymers, 16(23), 3268. https://doi.org/10.3390/polym16233268

Tarani, E., Arvanitidis, I., Christofilos, D., Bikiaris, D. N., Chrissafis, K., & Vourlias, G. (2023). Calculation of the degree of crystallinity of HDPE/GNPs nanocomposites by using various experimental techniques: a comparative study. Journal of Materials Science, 58(4), 1621–1639. https://doi.org/10.1007/s10853-022-08125-4

Ullah, S., & Ali, M. (2025). Development and properties investigation of recycled plastic solid interlocking blocks. Case Studies in Construction Materials, 23, e05342. https://doi.org/10.1016/j.cscm.2025.e05342

Yan, J., Zheng, Y., Zhou, Y., Liu, Y., Tan, H., Fu, Q., & Ding, M. (2023). Application of infrared spectroscopy in the multiscale structure characterization of poly(l-lactic acid). Polymer, 278, 125985. https://doi.org/10.1016/j.polymer.2023.125985

Yong Quek, C., Thung Calista, N. H., Chai, J. Y., Ye Lee, Z., Khaw, M. Y., Ting, C. H., Koay, S. C., & Chan, M. Y. (2025). A Comparative Study in Fused Filament Fabrication using Commercial and Recycled High-Density Polyethylene. Journal of Physical Science, 36(3), 1–14. https://doi.org/10.21315/jps2025.36.3.1